Relationship between the electronic structure of embedded single to triple atomic monolayers and bulk alloys

W. Olovsson,[1] E. Holmström,[2] J. Wills,[2] P. James,[3] I. A. Abrikosov,[4] and A. M. N. Niklasson[2]
[1]*Condensed Matter Theory Group, Department of Physics, Uppsala University, SE-751 21 Uppsala, Sweden*
[2]*Theoretical Division, Los Alamos National Laboratory, Los Alamos, New Mexico 87545, USA*
[3]*SKF Group Manufacturing Development Centre-MDC, SE-415 50 Göteborg, Sweden*
[4]*Department of Physics & Measurement Technology, Linköping University, SE-581 83 Linköping, Sweden*
(Received 16 June 2005; revised manuscript received 17 August 2005; published 18 October 2005)

The relation between the electronic structure of thin film nanosandwiches and bulk alloys has been investigated by means of first-principles electronic structure theory. The spin magnetization, layered projected spectral properties, and interface core-level shifts of Cu, Ni, Co, and Fe systems have been calculated. In order to compare thin films to bulk alloys, systems with equal average nearest-neighbor coordination have been compared. We find that the spin magnetization and interface core level shifts are closely related to bulk with the exception of the core level shifts in the Fe/Cu multilayers, which are more sensitive to the specific structure of the thin film geometry. The discrepancy is discussed in terms of interacting interface states in the Cu spacer. The experimental possibility of detecting embedded monolayers is also investigated.

DOI: 10.1103/PhysRevB.72.155419 PACS number(s): 73.22.−f

I. INTRODUCTION

Refined techniques for growing high-quality nanodevices such as magnetic multilayers and superlattices have created fascinating opportunities in materials science. The properties of these materials originate in the introduction of interfaces and the resulting quantum interferences between these interfaces. From a technological point of view this is of much interest since these systems offer possibilities of designing new magnetic and optical properties by changing the geometry of the interfaces. However, to analyze layered magnetic systems in detail, theoretically or experimentally, is difficult.

Bulk alloy systems is, on the other hand, a fairly well investigated field and a question to be answered is if it is possible to make predictions about the properties of layered metallic systems from bulk alloys. It has been shown that the behavior of the magnetic interface moments of 3*d* transition metal interfaces can be understood in terms of the magnetization of the corresponding binary bulk alloys.[1] Moreover, it is known that the magnetization of ordered compounds is, usually, very well described by their disordered alloys.[2] These studies indicate that it may be possible to predict and understand properties of layered materials from what is known about their disordered phase in bulk alloys. On the other hand, it is also known that many properties of layered systems depend on details of the electronic structure that are specific for their two-dimensional geometries—in particular the oscillatory magnetic interlayer coupling and the giant magnetoresistance.[3,4] It is thus of great interest to know to what extent properties of bulk alloys govern the specific features of thin film materials and what properties are unique due to the interfaces and quantum interference. In this paper we will perform a study of the relation between the electronic structure of embedded single to triple atomic monolayers and the corresponding binary bulk alloys. As the common parameter in the comparison between the thin film nanodevices and the alloys we choose the nearest-neighbor coordination of the atoms in the embedded films. This choice of order parameter allows a direct comparison with disordered alloys where the average nearest-neighbor coordination is determined by the atomic concentration. In this way we can analyze differences originating from higher order correlation (second-nearest-neighbor and more long-range ordering) effects specific for the thin film geometry and thereby elucidate similarities as well as discrepancies between the electronic structure of the thin films and the bulk alloys. It should be noted that this approach is adapted to local properties and would not be useful for studying global properties such as, e.g., transport.

One well used way of studying bonding and electronic structure in solids and at surfaces, as well as for molecules, is to measure the difference in core-electron binding energies, or core-level shift (CLS), as it is very sensitive to the local chemical environment of a specific atom. Experimentally, it is readily given by means of the x-ray photoelectron spectroscopy technique. This seem to make CLS an ideal method for a closer study of the properties of thin embedded films as compared to bulk alloys, although actual experimental setups could present difficulties of their own. Here we propose the introduction of interface core level shifts (IF-CLSs) to analyze properties specific to thin film geometries in analogy to the application in surface physics.[5–9]

In Sec. II we give some calculational details on the electronic structure methods that have been used. In Sec. III the relations between the spin magnetization, spectral properties and interface core-level shifts of thin embedded films and the corresponding bulk alloys are investigated and in Sec. IV the experimental detectability and spectral resolution of embedded layers are discussed.

II. CALCULATIONAL DETAILS

The electronic structure has been calculated self-consistently within the framework of density functional

theory[10,11] in a local density approximation.[12,13] The calculational methods are based on a scalar relativistic spin polarized linearized-muffin-tin-orbital method[14–18] and the corresponding Green's function technique for surfaces and interfaces.[19] The surface Green's function is constructed by means of the principal layer technique.[18,20–22] The broken translational symmetry perpendicular to the interfaces is treated within the interface Green's function technique, which does not rely on a slab or supercell geometry. The method is especially well suited for closed packed systems since the atomic sphere approximation is used. Alloys have been treated in the framework of the coherent potential approximation (CPA), and the details relevant for the present implementation can be found in Refs. 23 and 24. Dilute alloys have in the theoretical treatment been approximated by atomic concentrations of 1–2 %.

The thin film nanosystems investigated in the present study consist of a 1–3 monolayers (ML) thick slab of material A, embedded between two semi-infinite crystals of material B, which are put together to form a $B/A/B$ sandwich. Far away from the interface the electronic structure will be equal to the corresponding bulk B material. The width of the region for charge and spin relaxation surrounding the $B/A/B$ interface was chosen to be between 5 and 7 monolayers on each side of the interface.

A. Spectral properties

The spectral properties of the interface and bulk systems are investigated by means of the spectral density function

$$D^{\sigma}(\mathbf{k},E) = -\frac{1}{\pi}\,\mathrm{Im}\,\mathrm{Tr}G^{\sigma}(\mathbf{k},E), \tag{1}$$

calculated from the Green's function $G^{\sigma}(\mathbf{k},E)$ of spin σ, wave vector $\mathbf{k}$, and energy E. The layer, atomic or spin resolved spectral density are obtained by restricting the trace to single atomic layers, atomic sites or spin channels. When integrated over the two- (layer resolved) or three-(bulk) dimensional Brillouin zone the k-resolved spectral density yields the total density of states (DOS).

B. Core level shifts

There are different methods of calculating core-level shifts. Here we employ the complete screening picture, which includes both initial state (core-electron energy eigenvalue) and final state (energy relaxation) effects, in the same scheme. It was first used to calculate the shift between a free atom, and the atom in a metal.[5] Thereafter it has been successfully applied to both bulk[25,26] and surface core level shifts.[7,27] An advantage of the complete screening picture is that the problem of calculating core level shifts is not separated into independent calculations of initial and final state effects; both of these contributions are included simultaneously, and within the same scheme. The reference for the core level shift is in principle arbitrary, but for practical and comparison reasons usually chosen to be the pure metal system.

The most important quantity to calculate in this model is the generalized thermodynamic chemical potential of the core-ionized atoms, which is given by

$$\mu = \left.\frac{\partial E_{\mathrm{tot}}}{\partial c}\right|_{c\to 0}. \tag{2}$$

Here E_{tot} represents the total energy of a system where a specific core-electron of a particular atom has been ionized, with a total concentration c of ionized atoms. The $c\to 0$ limit is taken via extrapolation of the E_{tot} calculated at some finite concentrations. Calculations of Eq. (2) for each particular layer can be done separately. The method is easily generalized to different kinds of binding energy shifts, the interface core level shift (IF-CLS) studied in the present work is given by the difference of the generalized chemical potentials in the bulk of the pure metal μ_{bulk} and in the corresponding interface-layer $\mu_{\mathrm{IF\ layer}}$,

$$E_{\mathrm{IF\text{-}CLS}} = \mu_{\mathrm{IF\ layer}} - \mu_{\mathrm{bulk}}. \tag{3}$$

The complete screening picture is more complex as compared to the initial state approach, because calculations need to be done for different concentrations of ionized atoms c. It is, however, substantially more reliable. Also note that total energies rather than energy eigenvalues are used to compute the shifts. This is important because the underlying theory for our calculations is the density functional theory[10,11] (DFT) which, strictly speaking, is a theory for calculating total energies. However, another way to calculate CLS is to use the transition state model,[28,29] which also includes initial and final state effects. It was recently shown that the complete screening picture and the transition state model give very similar results for bulk alloys.[30] It has earlier been shown in Ref. 31 that Eq. (2) is a proper way of obtaining chemical potentials inside the formalism of the CPA single-site approximation.

III. RELATION BETWEEN THIN FILMS AND ALLOYS

A. Spin magnetization

An atom A of a layer embedded in some host material B is surrounded by n_A number of A atoms and, n_B number of B atoms in its nearest-neighboring shell. If we neglect parts of the correlation effects due to the ordering of the atoms at the interface, we may regard the A atoms at the interface as the average A atom of a disordered A_xB_{1-x} alloy with the atomic concentration x determined by

$$x = \frac{n_A}{n_A + n_B}. \tag{4}$$

This relation can be used to compare the properties between thin films and alloys. In Fig. 1 we show the magnetic moment of bulk alloys (dashed lines) and embedded thin films (symbols) as a function of average valence Z. The thin films are different monolayers and double layers of Fe, Co, and Ni embedded in fcc Cu, and the average number of valence electrons Z is determined by

$$Z = xZ_A + (1-x)Z_{\mathrm{Cu}} \quad (A = \mathrm{Fe,Co,Ni}), \tag{5}$$

where Z_A and Z_{Cu} are the valence of the embedded materials A and Cu host, respectively. The concentration x is calculated according Eq. (4), where n_A and n_B depend upon the orien-

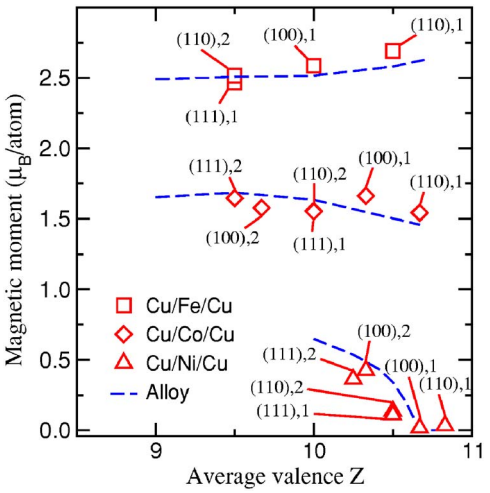

FIG. 1. (Color online) The individual magnetic spin moments as a function of the average number of valence electrons for the layered systems (full symbols) and corresponding bulk alloys (dashed lines). The indices at the layer points indicate the fcc interface normal directions and the number of embedded layers, respectively.

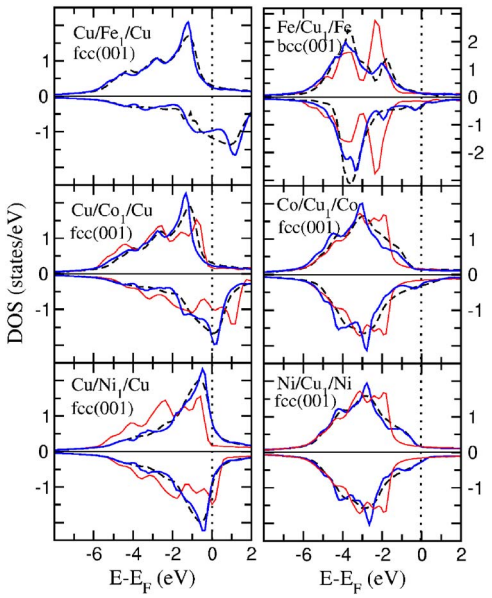

FIG. 2. (Color online) The layered resolved DOS of embedded monolayers (thick lines) and the atomic projected DOS of the corresponding bulk alloys (dashed lines) with an atomic concentration determined by the nearest-neighbor coordination of the thin film. As a comparison the DOS for the pure bulk material is displayed (thin lines).

tation of the interfaces and the thickness of the thin films (1 or 2 monolayers). The resemblance between the Slater-Pauling-like curve of the A_xCu_{1-x} alloys and the corresponding spin magnetization curve of the embedded layers, as is found in Fig. 1, clearly elucidate the close relation between the embedded films and the bulk alloys.

In the case of the Cu/Fe/Cu fcc interface system we find a slightly increased Fe moment as a function of increased number of Cu atoms in the first coordination shell, which follows the same trend as in the case of the corresponding bulk alloy. The graph does not show the magnetization for Fe concentrations lower than 30%. In that concentration range a high-spin to low-spin transition occurs[2] and the pure fcc Fe crystal as well as layered systems of Fe/Cu have a very complex magnetic behavior[32,33] and are therefore excluded from the present study.

For the Cu/Co/Cu interface systems we also have a good agreement between the spin magnetization of the embedded films and the bulk alloys. The number of Cu atoms in the nearest-neighboring shell has a rather small influence on the magnetic moment of Co. In the case of high concentration of Cu a small decrease is found for the Co moment.

For the embedded Ni films a transition to a low-spin state occurs when the number of nearest Ni atoms is less than ~6. This transition is also seen in the Ni_xCu_{1-x} alloys with an atomic concentration x around 50%.

Deviations between the magnetization of the thin films and bulk alloys in Fig. 1 can be explained in terms of multiple scattering effects in the thin films, which can give rise to quantum-well states.[34–36] Quantum interference states are shown to give rise to small shifts in the magnetic moment of thin embedded films.[37] In cases where a material has competing magnetic and nonmagnetic states the magnetic quantum-well states can even induce the onset of magnetism[38] or quench magnetism.[39] In the case of disordered alloys such effects are smeared out.

It is interesting to note the very small difference between the magnetic moment for a single embedded fcc(111) monolayer and the double fcc(110) monolayer seen in Fig. 1. These systems have the same coordination (corresponding to 50% atomic concentration for the bulk alloys) and are therefore expected to have a very similar magnetic moment. This is also in excellent agreement with the calculated moments of the thin films. Almost no shift at all is visible for the Co and Ni systems, while a small shift is seen for the Fe moments.

The conclusion from the overall agreement between the spin magnetization of bulk alloys and thin embedded films is thus that the film geometry seems to be less important for the magnitude of the magnetization in the studied cases. Of major importance is the coordination of the nearest-neighboring shell, a relation which is usually found also between ordered compounds and their alloys.[2] The spin magnetization of bulk alloys can therefore be used to estimate the magnetic behavior of thin films if the alloy concentration is determined by the nearest-neighbor coordination of atoms in the embedded film.

B. Spectral properties

In Fig. 2 the differences between the electronic structure of embedded layers and the corresponding bulk alloys is illustrated. Displayed is the layered and spin-resolved density of states (DOS) for single monolayers of Fe, Co, and Ni embedded in Cu fcc(001), and monolayers of Cu embedded in Fe bcc(100), Co fcc(100), and Ni fcc(100) (thick lines), together with the atomic projected DOS for the corresponding bulk alloys (dashed lines) with their concentration determined by the interface coordination, Eq. (4). For a comparison we also show the DOS of the pure elements in bulk (thin

lines). As is clearly seen from Fig. 2 the DOS for bulk alloys reproduces the main spectral characteristics of the embedded monolayer films (remarkably well for the majority band). Due to the disorder in the randomly distributed bulk alloy the spectral properties are smeared out compared to the thin films, which have more details in their spectral structures. Integrated properties such as charge, magnetic moment, and the hyperfine fields can, for that reason, be expected to be more similar than properties determined by the DOS at the Fermi level, such as the magnetic susceptibility and anisotropy or the electric conductivity. However, as mentioned above, under certain circumstances quantum-well states at the Fermi level can give rise to substantial magnetic effects.

The different behavior of the magnetic spin moment of Fe, Co, and Ni, in the thin films as well as bulk alloys, can be analyzed by the bandwidth of the elements (Figs. 1 and 2). The bandwidth decreases when going from Fe to Ni, i.e., the localized character of the electrons increases with increasing band filling. This is also seen for other transition metals. Another entity that affects the bandwidth is the coordination number of the atoms; a reduced coordination decreases the bandwidth due to reduced hybridization. The atoms in thin films and especially dilute alloys have a low coordination number and, thus, a more narrow bandwidth than the pure elements. In Ni, the narrowing of the bandwidth of the almost filled Ni bands reduces the DOS at the Fermi level, and the magnetic moment is quenched. Co and Fe, on the other hand, have less filled bands and the DOS at the Fermi level therefore does not decrease and Co and Fe therefore remain ferromagnetic. The qualitative behavior of the spin magnetization, both for the investigated thin films as well as for the bulk alloys, can thus be understood from the interplay between the band filling and the coordination. The same arguments may therefore hold also for other systems of transition metals.

In Fig. 3 we investigate the layer resolved DOS of the embedded monolayers (thick lines) with the DOS of double layers (dashed lines) as well as with the atomic projected DOS of the 1% dilute alloys (thin lines). It is worthwhile remarking that intermediate configurations, such as, for example, interface steps or partially mixed monolayers, are not taken into account in the present analysis.[40–43]

Comparing the DOS of the monolayers with the dilute cases in Fig. 3 we find that the embedded Fe, Co, and Ni monolayers and bilayers have somewhat wider bandwidths and more spectral structures. The difference in bandwidths can be explained, as described above, by the higher coordination of the monolayers compared to the dilute alloys. The majority spin channel of the Fe layer embedded in Cu fcc(001) has a structure that is very similar to the dilute case. In the case of the Cu monolayer embedded in Fe bcc(001) we also find a considerable resemblance with the dilute alloy. This is to be expected from the fact that all nearest-neighbor atoms of a Cu atom in the embedded bcc(001) film are Fe atoms. The most characteristic difference is the peak at about 2 eV below the Fermi level in the Fe minority spin channel which is absent in case of the dilute alloy. For the embedded Cu monolayer in Co or Ni the DOS of the Cu majority spin channel is very close to the dilute case, whereas the main peak of the DOS of the minority spin channel is somewhat shifted towards higher energies.

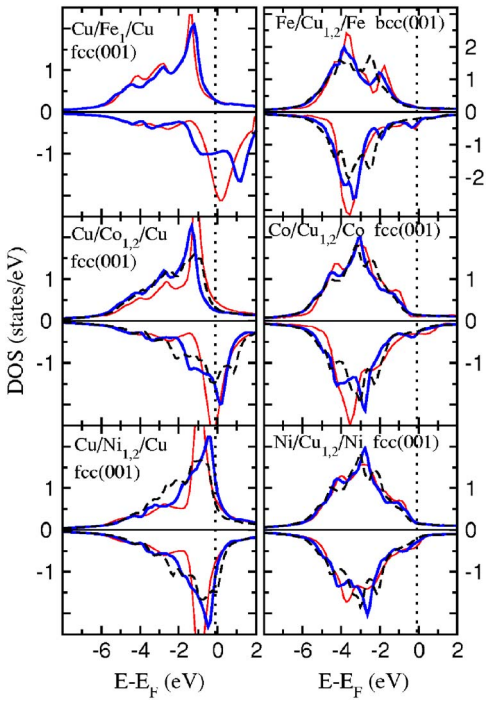

FIG. 3. (Color online) The layered resolved DOS of embedded monolayers (thick lines), the atomic projected DOS of the dilute alloy (thin lines), and the layered resolved DOS of double layers (dashed lines).

Comparing the DOS of the monolayers with the double layers we find an increased number of pronounced peaks and a somewhat broader and more bulklike DOS for the double layers. This can be explained as an effect of multiple scattering states, which give rise to more spectral peaks for the double layer,[38] and the increased coordination of the surrounding atoms of the same kind, which gives rise to more bulklike spectral properties.

C. Interface core-level shifts

In this section we investigate the $2p_{3/2}$ interface core-level shifts for the embedded Cu layers in the same fashion as for the magnetic moments and DOS above. In Table I the bulk alloy shifts are displayed. The calculations were performed for two different volumes, the theoretical equilibrium volume per atom of the magnetic metal host (Ni, Co, or Fe), denoted V_{magn} and the theoretical equilibrium volume per atom of the alloy, denoted V_{alloy}. The volume induced shift for pure Cu for the three different cases in Table I are 0.20 eV for Cu in the volume of Ni, 0.19 eV for Cu in the Co volume, and 0.07 eV for Cu in the bcc structure and volume of Fe.

The results from the direct calculations of the interface core-level shifts according to Eq. (3) are displayed in Table II. The calculations were performed by assuming the V_{magn} volumes.

In Fig. 4 we compare the V_{magn} core level shifts from Tables I and II by comparing the IF-CLS with the corresponding bulk alloy shifts. The local concentration is calculated according to Eq. (4). For both one and two Cu layers there is only a single shift due to symmetry and for three

TABLE I. Bulk CLS for Cu $2p_{3/2}$ in fcc $Cu_{1-x}Ni_x$, fcc $Cu_{1-x}Co_x$, and bcc $Cu_{1-x}Fe_x$ alloys, at fixed lattice constants corresponding to the theoretical values for the pure ferromagnetic bcc Fe, fcc Co, and fcc Ni metals (V_{magn}) and at the respective alloys equilibrium volumes (V_{alloy}).

Alloy	V_{magn} (Å^3)	Shift (eV)	V_{alloy} (Å^3)	Shift (eV)
$Cu_{100}Ni_0$	10.57	0.20	11.34	0.00
$Cu_{67}Ni_{33}$	10.57	−0.08	11.04	−0.18
$Cu_{33}Ni_{67}$	10.57	−0.22	10.80	−0.27
$Cu_{100}Co_0$	10.62	0.19	11.34	0.00
$Cu_{67}Co_{33}$	10.62	0.04	11.09	−0.06
$Cu_{33}Co_{67}$	10.62	0.02	10.85	−0.02
$Cu_{100}Fe_0$	10.99	0.07	11.34	0.00
$Cu_{50}Fe_{50}$	10.99	0.06	11.30	−0.00
$Cu_{10}Fe_{90}$	10.99	−0.03	11.10	−0.05
$Cu_{05}Fe_{95}$	10.99	−0.04	11.04	−0.06

layers there are two shifts: one that corresponds to the interface atoms (larger symbol) and one for the center atom (smaller symbol). In the fcc structures the Cu concentrations calculated from Eq. (4) are 33 and 66 % for 1 and 2 ML, respectively, and 66 and 100 % for the interface and center atoms in the 3 ML case. For bcc the corresponding concentrations are 0, 50, and 50/100 %, respectively.

In the figure we can see that the Cu IF-CLS in Ni and Co are well described by the alloy and the agreement is within 0.1 eV for all Cu thicknesses. For the Cu in Fe system, on the other hand, we see a large discrepancy between the IF-CLS as described by the alloy compared to the embedded nanosandwich. In the 1 ML case even the sign of the shifts is different.

One possibility for this behavior could be that since Fe is a weak ferromagnet, there could be anomalous magnetic moments in the interface Fe layers that could affect the CLS.[44] However, we have not found any magnetic moments in the multilayer system that could not be described by the corresponding bulk alloy magnetization. Therefore we find it unlikely that such magnetic effects could influence the CLS. This discrepancy may also come from several effects in the Cu spacer. For example, multiple scattering can give rise to quantum well states in this system that may change both the shape of the DOS and its intensity at the Fermi level.[37,45] At the same time there may be interface states present that interact when the slab thickness is small and change the DOS

TABLE II. Calculated IF-CLS for Cu $2p_{3/2}$ in 1–3 embedded layers. The V_{magn} lattice constants were used in the calculations.

Cu layers	fcc Ni	fcc Co	bcc Fe
1	−0.22	0.01	0.14
2	−0.07	0.05	0.25
3 inner	0.09	0.17	0.05
3 outer	−0.07	0.09	0.13

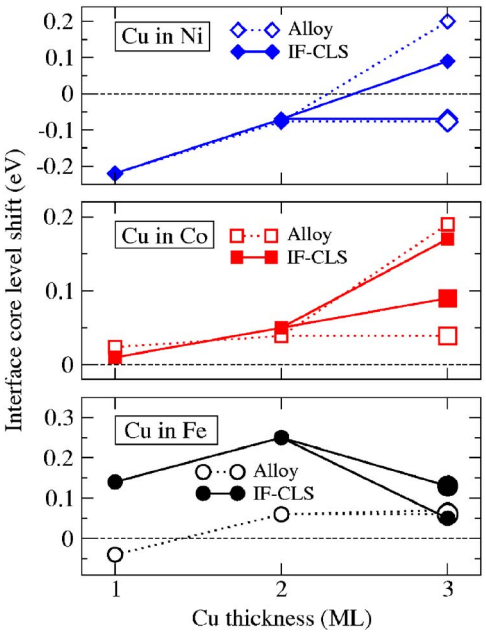

FIG. 4. (Color online) The interface core-level shifts (eV) for thin Cu layers (001) embedded in Ni, Co, and Fe (filled symbols) are compared to the effective bulk alloy shifts (open symbols). For 3 ML larger symbols denote outer layers. The crystal structures for the Cu in Ni and Cu in Co cases are fcc while the structure of the Cu in Fe calculation is bcc.

significantly.[45] If the DOS is changed at the Fermi level the screening properties are changed and the final state effects to the IF-CLSs are thus also changed.

In order to investigate the possibilities of interface states and quantum well states in the Fe/Cu/Fe trilayer we have performed a series of test calculations: If the magnetic alignment of the Fe layers is changed to be antiferromagnetic, the IF-CLS for the 2 ML system is still high (~0.19 eV) but if the magnetic moment of the interface Fe is constrained to be $1.0\mu_B$ and ferromagnetically aligned, the IF-CLS drops to about 0.08 eV. This should be compared to the same shift as described by the alloy that is 0.06 eV (see Table I). We also performed a calculation of the IF-CLS for the interface Cu layer in a $Fe/Cu_4/Fe$ system and there the value has dropped to 0.07 eV.

This indicates that the discrepancies between the IF-CLS for Fe/Cu/Fe as described by the alloy and the multilayer calculations is a result of interacting interface states for the thin slab thicknesses. If the effect was due to quantum well states there would also be a discrepancy for the 4 ML thickness [the period of the quantum well perturbations in the Fe/Cu/Fe system is ~2 ML (Refs. 37 and 45)]. Overall, the comparison between the effective bulk alloy shifts and the full calculations for the IF-CLS indicate that a part of the CLS in a multilayer is determined by the coordination number.

IV. DETECTABILITY OF EMBEDDED THIN FILMS

The quality of the embedded films is usually very sensitive to the preparation procedure and the interfaces may in-

termix at low temperatures.[46] Especially when measurements are performed on systems with single monolayers embedded in a host material it might be very risky to interpret the measured features as a result of the perfect single monolayer geometry. It is thus important to have a reliable tool for analyzing the quality of thin films. An element selective method is x-ray emission spectroscopy, which maps the layered projected partial DOS of the embedded film,[47,48] using dipole selection rules. This technique has also been extended to detect effects of spin polarization.[49–52] The x-ray spectroscopies are powerful techniques since they involve a localized core hole and are therefore element selective. However, it is not known if these techniques are sensitive enough to resolve structural differences of deeply embedded monolayers. For this purpose, one has to be able to detect and distinguish the specific spectral characteristics of an embedded single monolayer. Hence, the measured spectra of the embedded monolayer must differ from the double layer or from the dissolved layers forming an alloy. Without this ability it is not possible to trace the origin of features specific for "monolayer" systems.

From the result for the spectral characteristics in Sec. II B it seems possible to distinguish the characteristics of the embedded monolayers from double layers and dilute alloys. The differences are, however, not very large and a high resolution of the spectra is needed. Intermediate configurations, such as mixed layers or ensembles of monolayers and double layers, make the situation more intricate. Experimental techniques that cannot give the spin-resolved properties of embedded films will cause additional problems. Thus, in many cases, we have to rely on careful preparation procedures of the samples and/or a detailed comparison with calculations.[40]

V. SUMMARY

Different aspects of the relation between the electronic structure of thin films and bulk alloys, with their atomic concentration determined by the nearest-neighbor coordination of the atoms in the embedded films, have been investigated by means of first-principles electronic structure theory. Trends as well as magnitudes of the magnetic moments and interface core level shifts of the embedded thin films are found to be well described by the corresponding bulk alloys and less sensitive to the structure of the thin film geometry. In one of the studied cases, the interface core level shifts do not follow this rule and this is believed to be due to interacting interface states in the embedded Cu film. The qualitative behavior was explained in terms of band filling and coordination, both for the alloys as well as for the thin films. The main spectral properties of the thin films are also well described by the corresponding bulk alloys. However, the thin films have more pronounced peaks in the layered resolved DOS compared to the alloys but these are smeared out in the alloy due to disorder. This explains why an integrated property like the magnetic moment is well reproduced by the bulk alloy. Regarding the spectral detectability of embedded single monolayers we found characteristic differences in the layered resolved DOS compared to double layers as well as the dilute alloy. However, these differences are likely to be difficult to detect experimentally. Future high-resolution experimental efforts using, for example, shallow core levels are of great interest to enable a more detailed analysis of the structure of deeply embedded thin films.

ACKNOWLEDGMENTS

The authors are grateful for discussions with Dr. M. Magnuson. Financial support from the Swedish Research Council (VR) and the Swedish Foundation for Strategic Research (SSF) is acknowledged. Dr. Nicolas Bock is also acknowledged for fruitful discussions.

[1] A. M. N. Niklasson, B. Johansson, and H. L. Skriver, Phys. Rev. B **59**, 6373 (1999).
[2] P. James, O. Eriksson, B. Johansson, and I. A. Abrikosov, Phys. Rev. B **59**, 419 (1999).
[3] P. Grünberg, R. Schreiber, Y. Pang, M. B. Brodsky, and H. Sowers, Phys. Rev. Lett. **57**, 2442 (1986).
[4] M. N. Baibich, J. M. Broto, A. Fert, F. Nguyen Van Dau, F. Petroff, P. Eitenne, G. Creuzet, A. Friederich, and J. Chazelas, Phys. Rev. Lett. **61**, 2472 (1988).
[5] B. Johansson and N. Märtensson, Phys. Rev. B **21**, 4427 (1980).
[6] B. Johansson and N. Märtensson, Helv. Phys. Acta **56**, 405 (1983).
[7] M. Aldén, I. A. Abrikosov, B. Johansson, N. M. Rosengaard, and H. L. Skriver, Phys. Rev. B **50**, 5131 (1994).
[8] M. Aldén, H. L. Skriver, and B. Johansson, Phys. Rev. B **50**, 12 118 (1994).
[9] W. Olovsson, E. Holmström, A. Sandell, and I. A. Abrikosov, Phys. Rev. B **68**, 045411 (2003).
[10] P. Hohenberg and W. Kohn, Phys. Rev. **136**, B864 (1964).
[11] W. Kohn and L. Sham, Phys. Rev. **140**, A1133 (1965).
[12] D. M. Ceperley and B. J. Alder, Phys. Rev. Lett. **45**, 566 (1980).
[13] S. H. Vosko, L. Wilk, and M. Nusair, Can. J. Phys. **58**, 1200 (1980).
[14] O. K. Andersen, Phys. Rev. B **12**, 3060 (1975).
[15] H. L. Skriver, *The LMTO Method* (Springer-Verlag, Berlin, 1984).
[16] O. K. Andersen and O. Jepsen, Phys. Rev. Lett. **53**, 2571 (1984).
[17] O. K. Andersen, O. Jepsen, and D. Glötzel, *Highlights of Condensed-Matter Theory* (North Holland, New York, 1985).
[18] I. Turek, V. Drchal, J. Kudrnovský, M. Sob, and P. Weinberger, *Electronic Structure of Disordered Alloys, Surfaces and Interfaces* (Kluwer, Norwell, MA, 1997).
[19] H. L. Skriver and N. M. Rosengaard, Phys. Rev. B **43**, 9538 (1991).
[20] B. Wenzien, J. Kudrnovský, V. Drchal, and M. Sob, J. Phys.: Condens. Matter **1**, 9893 (1989).
[21] B. Velický and J. Kudrnovský, Surf. Sci. **21**, 93 (1977).
[22] J. Kudrnovský, P. Weinberger, and V. Drchal, Phys. Rev. B **44**, 6410 (1991).
[23] I. A. Abrikosov and H. L. Skriver, Phys. Rev. B **47**, 16 532

(1993).
[24] A. V. Ruban and H. L. Skriver, Comput. Mater. Sci. **15**, 119 (1999).
[25] I. A. Abrikosov, W. Olovsson, and B. Johansson, Phys. Rev. Lett. **87**, 176403 (2001).
[26] W. Olovsson, I. A. Abrikosov, and B. Johansson, J. Electron Spectrosc. Relat. Phenom. **127**, 65 (2002).
[27] M. Aldén, H. L. Skriver, and B. Johansson, Phys. Rev. Lett. **71**, 2449 (1993).
[28] J. F. Janak, Phys. Rev. B **18**, 7165 (1978).
[29] M. V. Ganduglia-Pirovano, J. Kudrnovský, and M. Scheffler, Phys. Rev. Lett. **78**, 1807 (1997).
[30] W. Olovsson, C. Göransson, L. V. Pourovskii, B. Johansson, and I. A. Abrikosov, Phys. Rev. B **72**, 064203 (2005).
[31] A. V. Ruban and H. L. Skriver, Phys. Rev. B **55**, 8801 (1997).
[32] V. L. Moruzzi, P. M. Marcus, and J. Kübler, Phys. Rev. B **39**, 6957 (1989).
[33] T. Asada and S. Blügel, Phys. Rev. Lett. **79**, 507 (1997).
[34] S. A. Lindgren and L. Walldèn, Phys. Rev. Lett. **59**, 3003 (1987).
[35] J. E. Ortega and F. J. Himpsel, Phys. Rev. Lett. **69**, 844 (1992).
[36] C. Carbone, E. Vescovo, O. Rader, W. Gudat, and W. Eberhardt, Phys. Rev. Lett. **71**, 2805 (1993).
[37] A. M. N. Niklasson, S. Mirbt, H. L. Skriver, and B. Johansson, Phys. Rev. B **53**, 8509 (1996).
[38] A. M. N. Niklasson, S. Mirbt, H. L. Skriver, and B. Johansson, Phys. Rev. B **56**, 3276 (1997).
[39] S. Mirbt, B. Johansson, and H. L. Skriver, Phys. Rev. B **53**, R13310 (1996).
[40] E. Holmström, L. Nordström, L. Bergqvist, B. Skubic, B. Hjörvarsson, I. A. Abrikosov, P. Svedlindh, and O. Eriksson, Proc. Natl. Acad. Sci. U.S.A. **101**, 4742 (2004).
[41] B. Skubic, E. Holmström, O. Eriksson, A. M. Blixt, G. Andersson, B. Hjörvarsson, and V. Stanciu, Phys. Rev. B **70**, 094421 (2004).
[42] A. M. N. Niklasson, I. A. Abrikosov, S. Mirbt, and B. Johansson, *Effects of Interface Intermixing on the Magnetic Interlayer Coupling* (Plenum, New York, 1997).
[43] J. Kudrnovský, V. Drchal, I. Turek, M. Sob, and P. Weinberger, Phys. Rev. B **53**, 5125 (1996).
[44] I. Turek, J. Kudrnovský, V. Drchal, and P. Weinberger, Phys. Rev. B **49**, 3352 (1994).
[45] A. M. N. Niklasson, L. Nordström, S. Mirbt, B. Johansson, and H. L. Skriver, J. Phys.: Condens. Matter **11**, 975 (1999).
[46] A. M. N. Niklasson, I. A. Abrikosov, and B. Johansson, Phys. Rev. B **58**, 3613 (1998).
[47] A. Nilsson *et al.*, Phys. Rev. B **54**, 2917 (1996).
[48] O. Karis, M. Magnuson, T. Wiell, M. Weinelt, N. Wassdahl, A. Nilsson, N. Mårtensson, E. Holmström, A. M. N. Niklasson, and O. Eriksson, Phys. Rev. B **62**, R16239 (2000).
[49] B. T. Thole, G. van der Laan, and G. A. Sawatzky, Phys. Rev. Lett. **55**, 2086 (1985).
[50] G. Schütz, W. Wagner, W. Wilhelm, P. Kienle, R. Zeller, R. Frahm, and G. Materlik, Phys. Rev. Lett. **58**, 737 (1987).
[51] P. Strange, P. J. Durham, and B. L. Györffy, Phys. Rev. Lett. **67**, 3590 (1991).
[52] L. C. Duda, J. Stöhr, D. C. Mancini, A. Nilsson, N. Wassdahl, J. Nordgren, and M. G. Samant, Phys. Rev. B **50**, R16758 (1994).